

Electronic Supplementary Information for:  
Release of gold (Au), silver (Ag) and cerium dioxide  
(CeO<sub>2</sub>) nanoparticles from sewage sludge incineration ash

Jonas Wielinski<sup>a,b</sup>, Alexander Gogos<sup>a,c</sup>, Andreas Voegelin<sup>a</sup>, Christoph R. Müller<sup>d</sup>,  
Eberhard Morgenroth<sup>a,b</sup> and Ralf Kaegi<sup>a\*</sup>

Submitted on June 1<sup>st</sup>, 2021, Accepted on September 9<sup>th</sup>, 2021

<sup>a</sup>Eawag, Swiss Federal Institute of Aquatic Science and Technology, 8600 Dübendorf, Switzerland

<sup>b</sup>ETH Zürich, Institute of Environmental Engineering, 8093 Zürich, Switzerland

<sup>c</sup>EMPA, Swiss Federal Laboratories for Materials Science and Technology, 9014 St. Gallen, Switzerland

<sup>d</sup>ETH Zürich, Institute of Energy Technology, 8092 Zürich, Switzerland

Corresponding author:

\*Ralf Kaegi, ralf.kaegi@eawag.ch, Tel.: +41 58 765 5273, Eawag, Überlandstrasse 133, 8600 Dübendorf, Switzerland.

This Electronic Supplementary Information document contains:

- 11 pages,
- 8 figures, and
- 1 table.

## Contents

S1 ENP characterization: electron microscopy and single particle ICP-MS. . . . .	S3
S2 Pilot WWTP setup . . . . .	S5
S3 Hydraulic parameter determination. . . . .	S6
S4 Ash grain size distributions. . . . .	S8
S5 Diameter of the < 10 kDa Au “nanoparticle” . . . . .	S9
S6 Comparison of bulk and single particle ICP-MS results . . . . .	S10

## List of Figures

S1 Au-NP characterization. . . . .	S3
S2 Ag-NP characterization. . . . .	S4
S3 CeO <sub>2</sub> -NP characterization.. . . . .	S4
S4 Schematic of the pilot wastewater treatment plant. . . . .	S5
S5 Conductivity signal experiment A.. . . . .	S6
S6 Conductivity signal experiment B. . . . .	S7
S7 Conductivity signal experiment C.. . . . .	S7
S8 Ash grain size distributions, experiments A-C. . . . .	S8

## List of Tables

S1 Comparison of concentrations determined by single particle and bulk ICP MS . . . . .	S10
---	-----

## S1 ENP characterization: electron microscopy and single particle ICP-MS

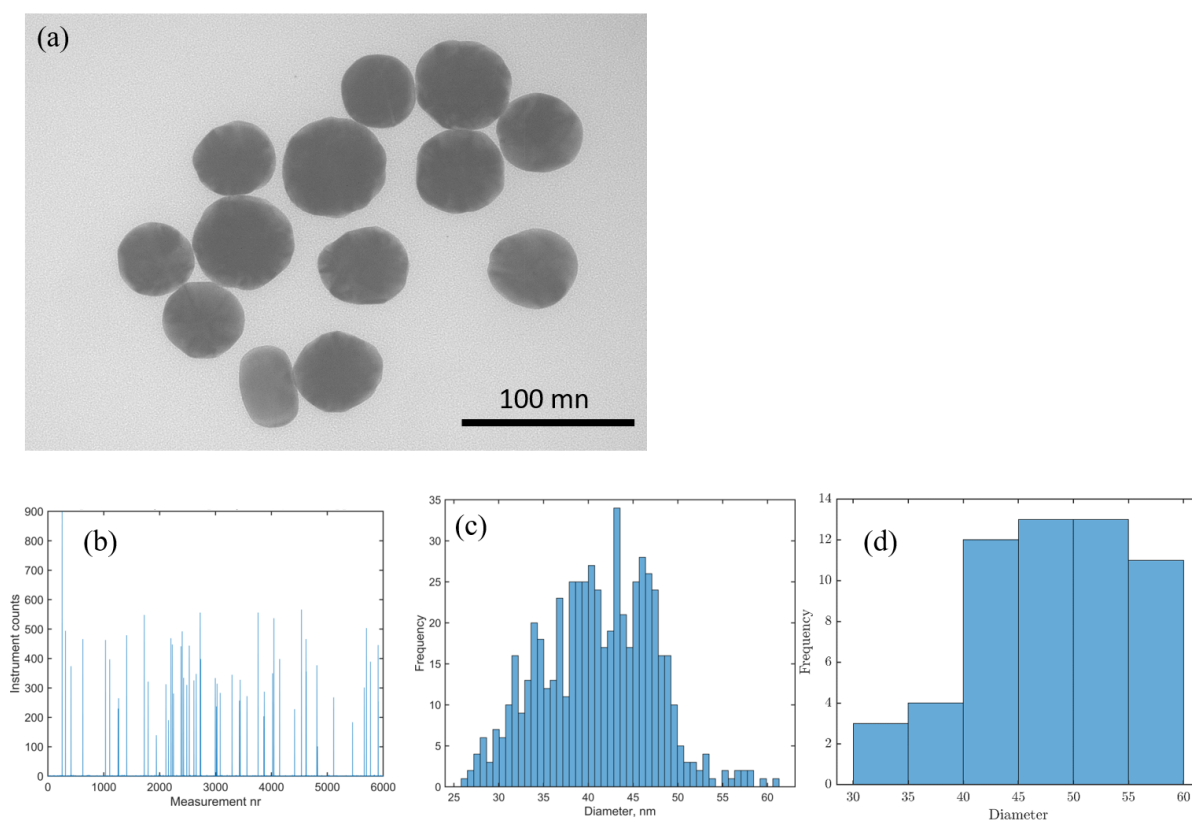


FIGURE S1. Characterization of Au-NP used for spiking. (a) Bright field-TEM image of the Au-NP that were spiked to the pilot wastewater treatment plant (WWTP). The image was recorded on a Hitachi HT7700 TEM with an acceleration voltage of 100.0 kV. (b) SpICP-MS instrument counts and (c) the corresponding histogram of counts converted into Au particle diameters according to Pace et al. (2011). The data is also indicated in Figure 5 in the main text. (d) Diameters of particles depicted in (a) and further TEM images of the Au-NP as determined by image analysis using Matlab.

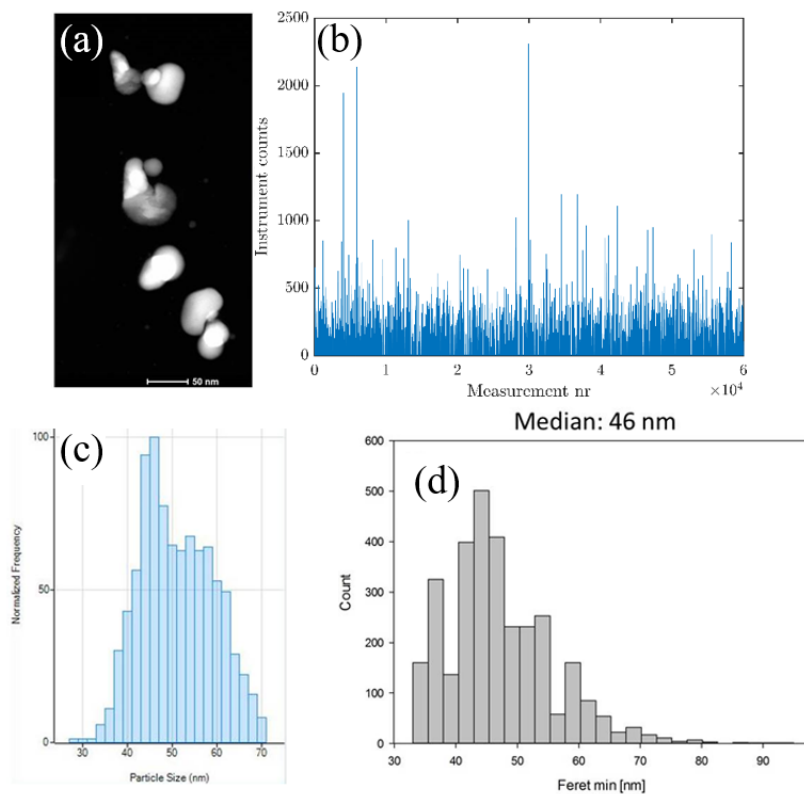


FIGURE S2. Characterization of the Ag-NP that were spiked to the pilot WWTP. (a) HAADF image (Talos, FEI), (b) spICP-MS instrument counts and (c) the corresponding histogram particle size distribution determined using the Nanocount module (Masshunter software, Agilent) (d) the diameter determined by the particle sizer plugin for imageJ (Wagner and Eglinger, 2017). Parts of the image have already been included in a previous publication (Gogos et al., 2019).

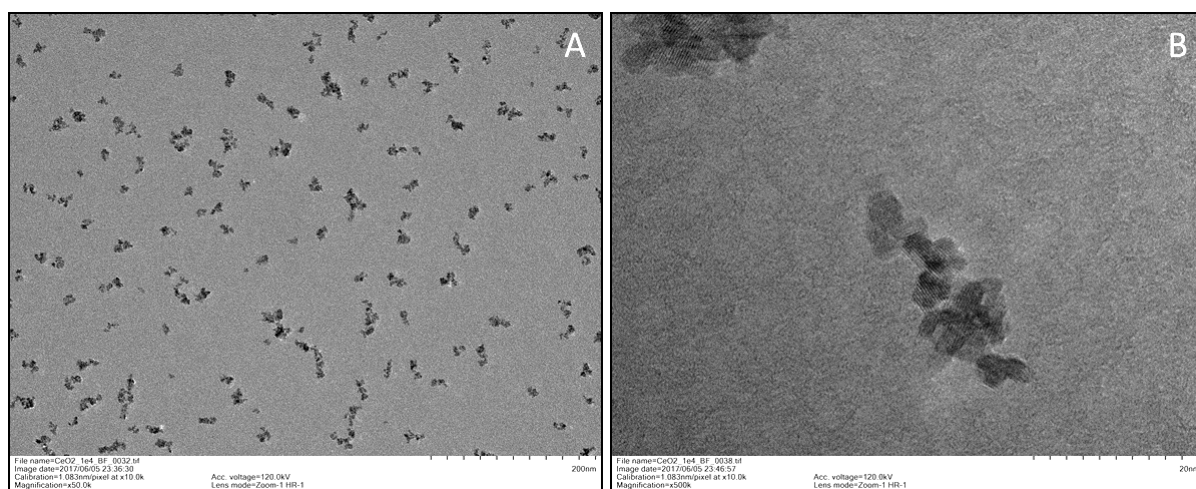


FIGURE S3. Characterization of the CeO<sub>2</sub>-NP by bright field-TEM. (A) particles at 50k magnification and (B) at 500k magnification. Both images were recorded on a Hitachi HT7700 TEM with an acceleration voltage of 120.0 kV.

## S2 Pilot WWTP setup

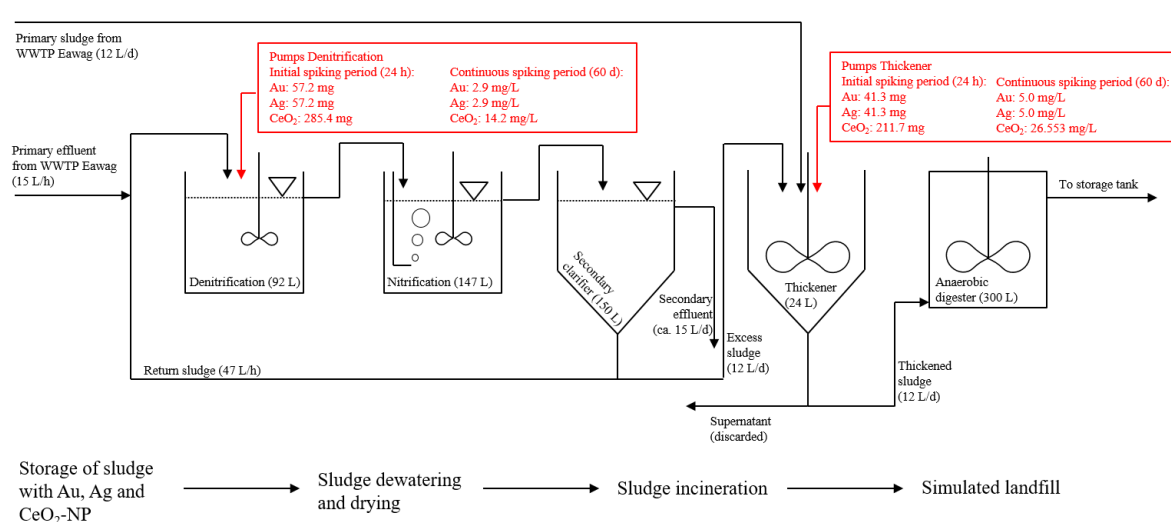


FIGURE S4. Schematic of the spiking setup used to prepare the spiked sludge and ash sample. For the initial spiking period (24 h) that was used to reach steady-state concentrations in the pilot WWTP, the total masses of Au, Ag and Ce spiked to the denitrification or thickener are given, whereas for the longer continuous spiking period (60 d), the concentrations in the spiking dispersions are given. Corresponding and complementary information is included in Table 1.

### S3 Hydraulic parameter determination

The conductivity data from the KCl tracer column experiments was evaluated using the 1-D solution of the advection-dispersion equation which can be applied to model conservative solute transport in saturated porous media resulting from an instantaneous source (Crank, 1979):

$$c(x, t) = \frac{N}{2A\epsilon\sqrt{\pi D_{\text{eff}}t}} \exp\left(-\frac{(x-ut)^2}{4D_{\text{eff}}t}\right) \quad (\text{S.1})$$

Where  $c$  is the conductivity,  $x$  the length of the column,  $t$  is the time after the injection of conductivity tracer,  $N$  a scaling parameter,  $A$  the cross section of the column,  $\epsilon$  the porosity of the ash in the packed column,  $D_{\text{eff}}$  the effective dispersion coefficient of the tracer in the column and  $u$  the velocity of the water in the ash column. Tubes were kept as short as possible and their influence to the dispersion was regarded as insignificant compared to the column.

The conductivity experiments were performed after the collection of the samples. The column was continuously fed with artificial rainwater. A pulse source of a 1 mM KCl solution was added via a loop connected to an Rheodyne injection valve.

Fitting parameters were  $N$ ,  $D_{\text{eff}}$  and  $u$ .  $N$  was allowed to vary in each replicate experiment, whereas  $u$  and  $D_{\text{eff}}$  were forced to a single value for all replicate experiments. Initial conditions were based on published data for the diffusivity of chloride in water ( $1.38 \cdot 10^{-9} \text{ m}^2/\text{s}$ ) (Tang and Sandall, 1985). Other initial conditions were chosen based on experience. Computation was done using Matlab.

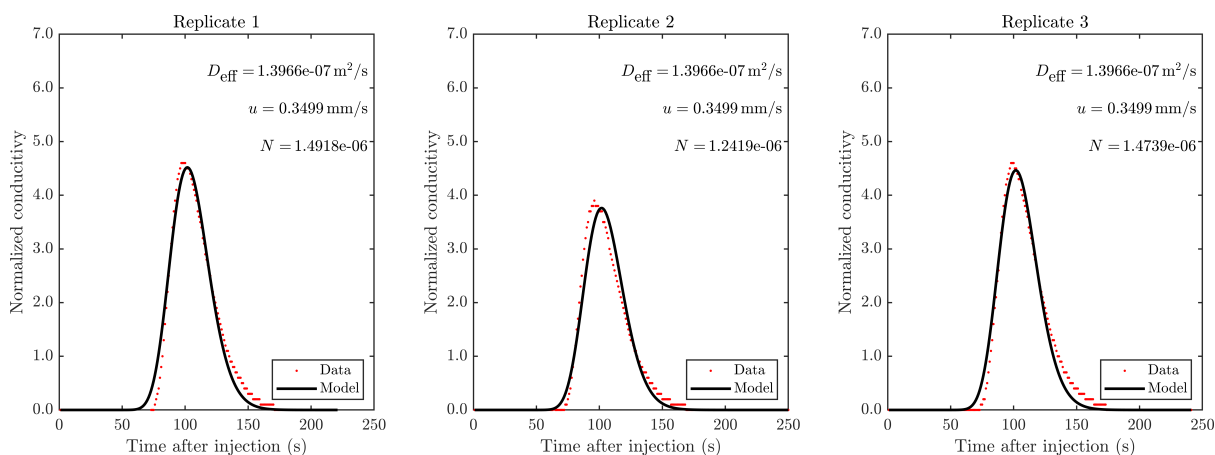


FIGURE S5. Conductivity signal (red dots) obtained on the column packed with ash of experiment “A”(spiking experiment) and the model calculations using the extracted parameters from the 1D solution of the advection-dispersion equation. The porosity was determined independently and included as a constant.

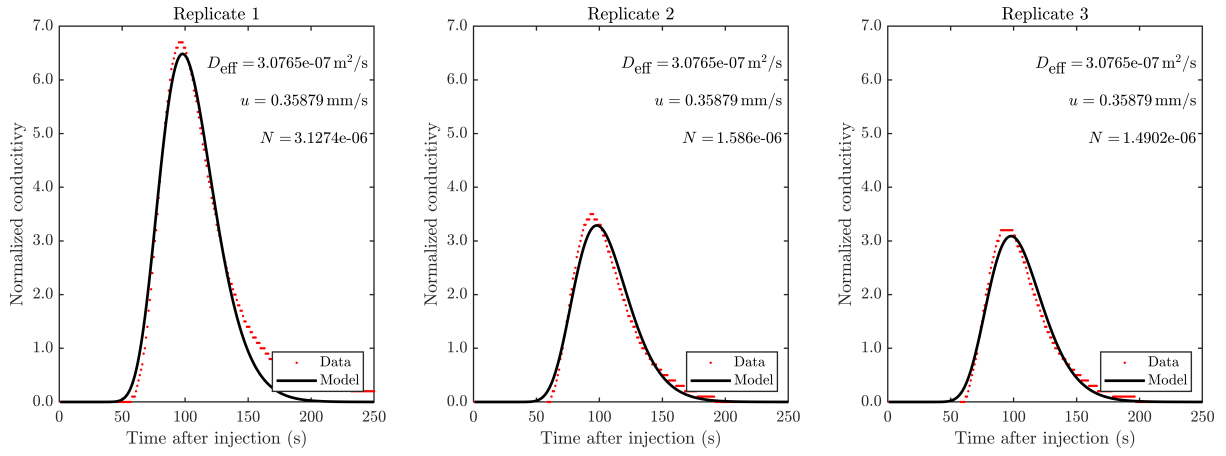


FIGURE S6. Conductivity signal (red dots) obtained on the column packed with ash of experiment “B”(WWTP Chiasso) and the model calculations using the extracted parameters from the 1D solution of the advection-dispersion equation. The porosity was determined independently and included as a constant.

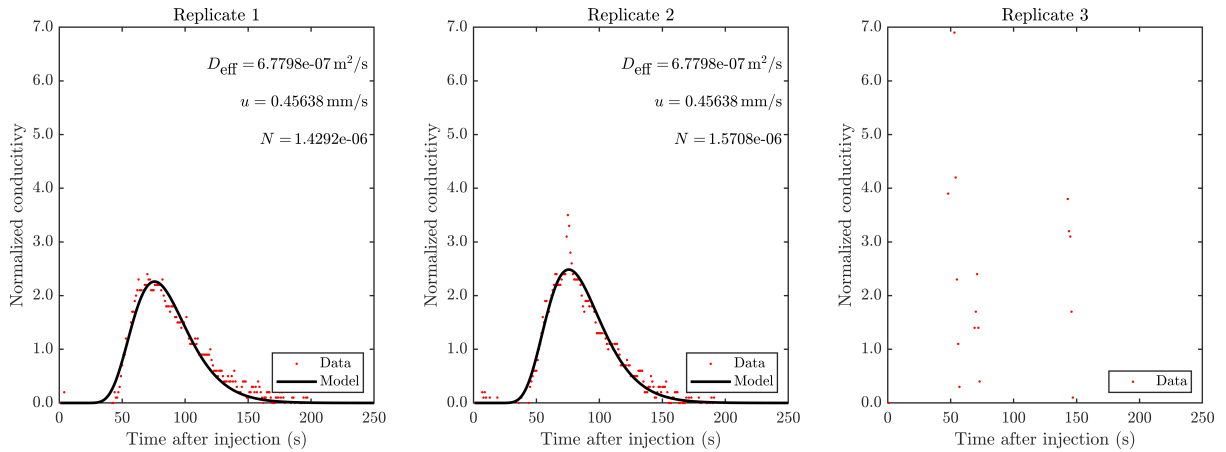


FIGURE S7. Conductivity signal (red dots) obtained on the column packed with ash of experiment “C”(WWTP La Chau-de-Fonds) and the model calculations using the extracted parameters from the 1D solution of the advection-dispersion equation. The porosity was determined independently and included as a constant. For experiment C, only two out of three recordings of the conductivity were successful and used to derive the  $D_{\text{eff}}$  and  $u$ .

## S4 Ash grain size distributions

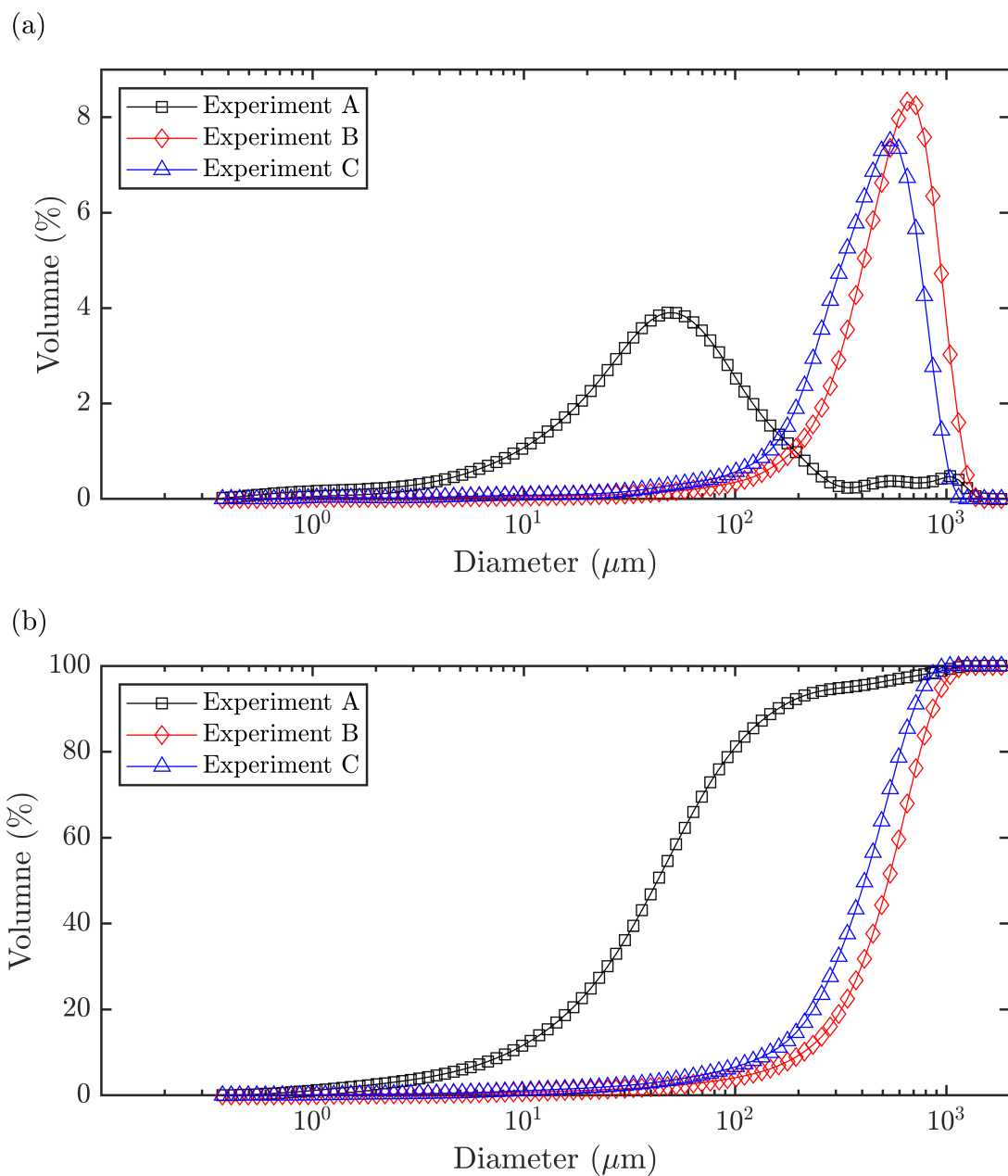


FIGURE S8. (a) Volume distribution (%) as a function of the diameter ( $\mu\text{m}$ ) and (b) cumulated volume distribution.



## S5 Diameter of the < 10 kDa Au “nanoparticle”

All particles weight  $\approx 10$  kDa or less. The atomic mass of Au is 197 Da, thus:

$$\frac{10^4}{197} \approx 51 \text{ Au atoms per particle} \quad (\text{S.2})$$

Au crystallizes in face centered cubic (fcc) unit cells with a unit cell edge length around 0.408 nm (Swanson, 1953). Each fcc unit cell consists of 14 atoms, but through the shared atoms, we must account each cell with 4 atoms.

$$\frac{51}{4} \approx 13 \text{ unit cells/particle} \quad (\text{S.3})$$

We find, assuming the particles to be spherical, that

$$\frac{V_{\text{particle}}}{V_{\text{unit cell}}} = 13 = \frac{4}{3} \frac{\pi r^3}{(0.408 \text{ nm})^3} \rightarrow r = \left( \frac{3 \cdot 13 \cdot (0.408 \text{ nm})^3}{4 \cdot \pi} \right)^{1/3} = 0.60 \text{ nm} \quad (\text{S.4})$$

Thus, the largest Au particle to pass the 10 kDa filter is around 1.20 nm in diameter.

## S6 Comparison of bulk and single particle ICP-MS results

TABLE S1. Total, particulate and dissolved Au concentrations as determined by single particle inductively coupled plasma mass spectrometry (spICP-MS, columns 2 to 4) and bulk ICP-MS (columns 5 to 7).

Fraction	spICP-MS			bulk ICP-MS		
	Au total ( $\mu\text{g/L}$ )	Au particulate ( $\mu\text{g/L}$ )	Au dissolved ( $\mu\text{g/L}$ )	Au total ( $\mu\text{g/L}$ )	Au particulate ( $\mu\text{g/L}$ )	Au dissolved ( $\mu\text{g/L}$ )
1	978.1	168.7	931.1	679.0	442.3	236.7
2	75.3	13.3	43.4	21.4	20.8	0.6
5	127.5	5.4	119.5	7.4	7.3	0.1
10	6.7	6.7	6.4	4.2	4.2	0.0
20	3.0	1.2	2.8	1.8	1.8	0.0
30	1.7	0.2	1.6	1.0	1.0	0.0
40	1.3	0.1	1.2	0.6	0.6	0.0

## References

- Crank, J. (1979). *The mathematics of diffusion*. Oxford University Press.
- Gogos, A., Kaegi, R., Wielinski, J., Matzke, M., Stahlmecke, B., Kaminski, H., Asbach, C., and Cornelis, G. (2019). Report the behavior of ENM in reactors. Report, Horizon 2020 NanoFASE Project.
- Pace, H. E., Rogers, N. J., Jarolimek, C., Coleman, V. A., Higgins, C. P., and Ranville, J. F. (2011). Determining transport efficiency for the purpose of counting and sizing nanoparticles via single particle inductively coupled plasma mass spectrometry. *Analytical Chemistry*, 83(24):9361–9369.
- Swanson, H. E. (1953). *Standard X-ray diffraction powder patterns*, volume 1. US Department of Commerce, National Bureau of Standards.
- Tang, A. and Sandall, O. C. (1985). Diffusion coefficient of chlorine in water at 25 – 60 °C. *Journal of Chemical & Engineering Data*, 30(2):189–191.
- Wagner, T. and Eglinger, J. (2017). thorstenwagner/ij-particlesizer: v1.0.9 snapshot release. *Zenodo*.